

Phase Frustration Induced Intrinsic Bose Glass in the Kitaev-Bose-Hubbard Model

Yi-fan Zhu¹ and Shi-jie Yang^{1,*}

¹*Department of Physics, Beijing Normal University, Beijing 100875, China*

We report an intrinsic “Bubble Phase” in the two-dimensional Kitaev-Bose-Hubbard model, driven purely by phase frustration between complex hopping and anisotropic pairing. By combining Inhomogeneous Gutzwiller Mean-Field Theory with a Bogoliubov-de Gennes stability analysis augmented by a novel Energy Penalty Method, we demonstrate that this phase spontaneously fragments into coherent islands, exhibiting the hallmark Bose glass signature of finite compressibility without global superfluidity. Notably, we propose a unified framework linking disorder-driven localization to deterministic phase frustration, identifying the Bubble Phase as a pristine, disorder-free archetype of the Bose glass. Our results provide a theoretical blueprint for realizing glassy dynamics in clean quantum simulators.

INTRODUCTION

Localization phenomena in quantum many-body systems remain a central theme in modern physics. Since the seminal proposal of Anderson localization [1], disorder has been identified as the key mechanism leading to wavefunction localization and insulating behavior. In the specific context of interacting bosons subject to such random potentials, Fisher *et al.* [2] established the concept of the “Bose Glass” (BG) as a gapless, compressible, yet insulating Griffiths phase. This phase has been experimentally realized in optical lattices using speckle potentials [3]. While the canonical BG is typically driven by diagonal disorder (random chemical potentials), subsequent studies have shown that off-diagonal disorder (random hopping amplitudes) can also induce similar glassy states [4–6], reinforcing the paradigm that extrinsic randomness is the prerequisite for glassiness.

However, recent research interests have shifted toward the frontier of disorder-free localization [7, 8]. A pivotal question is whether intrinsic mechanisms or lattice geometry alone can generate glass-like behavior or spatial fragmentation in clean systems. Significant progress has been made in systems governed by quasi-periodic potentials, exemplified by the celebrated Aubry-André model [9, 10] and incommensurate moiré superlattices [11], where deterministic incommensuration induces localization. Beyond quasi-periodicity, recent studies on commensurate twisted bilayers have revealed that geometric interference alone can drive the system into spatially modulated phases, featuring insulating islands embedded in a superfluid sea [12]. Furthermore, it has been demonstrated that strictly clean quasicrystals can host intrinsic Bose glass phases driven purely by geometric complexity [13].

Among possible intrinsic mechanisms, phase frustration induced by artificial gauge fields has been shown to generate rich quantum phases [14, 15]. While lattice geometry or interaction constraints typically lead to exotic *ordered* states—such as vortex lattices [14], supersolids [15], or chiral Mott insulators [16]—they can also fundamentally disrupt global phase coherence. Crucially,

under extreme conditions, frustration can force the system to relieve stress through spontaneous spatial fragmentation, stabilizing a glassy state that is intrinsic and deterministic.

Recently, bosonic analogues of the Kitaev model—featuring both complex hopping and explicit pairing—have garnered significant attention, particularly following their experimental realizations in one-dimensional optomechanical [17] and superconducting circuit platforms [18]. While these studies have revealed rich physics such as chiral transport and Majorana-like correlations [19–21], they have been predominantly confined to chains or ladders. In this Letter, we generalize this framework to two dimensions, where the orbital magnetic flux emerges as a decisive degree of freedom. Taking the rational flux $\alpha = 1/16$ as a representative example, we report that the intrinsic phase frustration arising from the interplay between the Peierls phases and the anisotropic Kitaev pairing drives the system into a robust “Bubble Phase.” This phase exhibits the hallmark macroscopic characteristics of a Bose glass: it is compressible ($\kappa > 0$) and possesses a finite density of states, yet remains globally insulating due to spontaneous spatial fragmentation.

MODEL

We consider interacting bosons on a two-dimensional square lattice driven by artificial gauge fields. The system is described by the Kitaev-Bose-Hubbard Hamiltonian:

$$\hat{H} = - \sum_{\mathbf{r}} \sum_{\nu=x,y} \left(J e^{i\theta_{\mathbf{r},\mathbf{r}+\hat{\nu}}} \hat{b}_{\mathbf{r}}^\dagger \hat{b}_{\mathbf{r}+\hat{\nu}} + \Delta e^{i\phi_{\mathbf{r},\mathbf{r}+\hat{\nu}}} \hat{b}_{\mathbf{r}}^\dagger \hat{b}_{\mathbf{r}+\hat{\nu}}^\dagger + \text{H.c.} \right) + \frac{U}{2} \sum_{\mathbf{r}} \hat{n}_{\mathbf{r}} (\hat{n}_{\mathbf{r}} - 1) - \mu \sum_{\mathbf{r}} \hat{n}_{\mathbf{r}}, \quad (1)$$

where $\hat{b}_{\mathbf{r}}$ ($\hat{b}_{\mathbf{r}}^\dagger$) are bosonic annihilation (creation) operators at site $\mathbf{r} = (x, y)$, and $\hat{n}_{\mathbf{r}}$ is the number operator. The system is characterized by the hopping amplitude J and the pairing amplitude Δ , dressed by the Peierls phases θ and ϕ , respectively.

We adopt the symmetric gauge $\mathbf{A} = \pi\alpha(-y, x, 0)$ to define the magnetic flux α per plaquette. The explicit Peierls phases for the bonds connecting \mathbf{r} and $\mathbf{r} + \hat{\nu}$ are given by:

$$\theta_{\mathbf{r}, \mathbf{r} + \hat{x}} = -\pi\alpha y, \quad \theta_{\mathbf{r}, \mathbf{r} + \hat{y}} = \pi\alpha x. \quad (2)$$

Crucially, we restrict our study to the case where the pairing phases strictly follow the gauge field, i.e., $\phi_{\mathbf{r}, \mathbf{r} + \hat{\nu}} = \theta_{\mathbf{r}, \mathbf{r} + \hat{\nu}}$.

This specific choice generates intrinsic phase frustration due to the distinct transformation properties of the kinetic and pairing terms under spatial inversion. For a generic bond along the direction $\hat{\nu}$, the kinetic term is directional: a particle hopping forward ($\mathbf{r} \rightarrow \mathbf{r} + \hat{\nu}$) picks up a phase $+\theta$, whereas the reverse process ($\mathbf{r} + \hat{\nu} \rightarrow \mathbf{r}$) picks up the conjugate phase $-\theta$. In contrast, the pairing term is bond-symmetric: the creation of a pair on the bond $(\mathbf{r}, \mathbf{r} + \hat{\nu})$ involves the same phase factor structure regardless of the bond orientation definition. This fundamental mismatch prevents the system from simultaneously minimizing the kinetic and pairing energies, driving the formation of the intrinsic Bubble Phase.

PHASE DIAGRAM

A. Method: Inhomogeneous GMFT

To explore the ground state properties of this two-dimensional frustrated system, we employ the Inhomogeneous Gutzwiller Mean-Field Theory (IGMFT) [22, 23]. The many-body wavefunction is approximated by a product of local states, $|\Psi_G\rangle = \prod_{\mathbf{r}} (\sum_{n=0}^{n_{\max}} f_{n,\mathbf{r}} |n\rangle_{\mathbf{r}})$, where $f_{n,\mathbf{r}}$ are the complex variational parameters satisfying the normalization condition $\sum_n |f_{n,\mathbf{r}}|^2 = 1$. The ground state is obtained by minimizing the energy functional $\langle \Psi_G | \hat{H} | \Psi_G \rangle$ via imaginary-time evolution, a standard procedure to reach the global energy minimum in the variational manifold.

While mean-field approaches neglect off-site quantum fluctuations, the choice of IGMFT is dictated by the specific computational challenges imposed by the Hamiltonian. Standard exact techniques face severe bottlenecks: the complex Peierls phases introduce a prohibitive sign problem for Quantum Monte Carlo (QMC), while the two-dimensional geometry imposes steep scaling costs for Density Matrix Renormalization Group (DMRG). IGMFT circumvents these limitations, providing a robust framework that naturally incorporates complex phases and explicitly resolves the spatially inhomogeneous order parameters essential for characterizing the Bubble Phase.

B. Phase Identification

The resulting ground state phase diagram for a representative flux $\alpha = 1/16$ is presented in Fig. 1. To rigorously distinguish the phases, we employ two complementary order parameters focusing on real-space connectivity and momentum-space coherence.

Real-space clustering.— To probe the connectivity of the superfluid regions, we utilize the Hoshen-Kopelman (HK) algorithm [24]. This technique performs a cluster analysis on the local order parameter field $\psi_{\mathbf{r}} = \langle \hat{b}_{\mathbf{r}} \rangle$. Defining two sites as “connected” if their correlation $|\psi_{\mathbf{r}} \psi_{\mathbf{r}'}|$ exceeds a threshold, the HK algorithm reveals three regimes [Fig. 1(a)]: (i) The **Mott Insulator (MI)**, where no clusters form; (ii) The **Superfluid (SF)**, characterized by a single percolating cluster; (iii) The **Bubble Phase**, an intermediate regime where finite-sized, disconnected superfluid clusters emerge but fail to percolate globally.

Momentum-space coherence.— To distinguish the Bubble phase from the Unstable Superfluid, we analyze the spectral structure of the order parameter. While the standard Inverse Participation Ratio (IPR) is typically defined for the density $n(\mathbf{k})$, here we utilize a modified *spectral IPR* calculated directly from the order parameter’s Fourier amplitude $|\tilde{\psi}_{\mathbf{k}}|$:

$$\mathcal{I}_{\mathbf{k}} = \frac{\sum_{\mathbf{k}} |\tilde{\psi}_{\mathbf{k}}|^2}{(\sum_{\mathbf{k}} |\tilde{\psi}_{\mathbf{k}}|)^2}. \quad (3)$$

Compared to the density-based IPR ($\sim \sum n_{\mathbf{k}}^2$), this amplitude-based measure provides superior sensitivity to the emerging coherence peaks against the diffuse background characteristic of the frustrated phases, yielding a sharper delineation of the phase boundaries in Fig. 1(b). The resulting map in Fig. 1(b) reveals a counter-intuitive feature: the deep Superfluid regime exhibits a *lower* $\mathcal{I}_{\mathbf{k}}$ compared to the Bubble Phase boundary. Detailed inspection of the momentum distribution shows that while the high-hopping phase retains a condensate peak, it is accompanied by a proliferation of diffuse background modes. This significant background weight—arising from chaotic spatial fluctuations (precursors to dynamical instability)—drastically suppresses the normalized ratio $\mathcal{I}_{\mathbf{k}}$. In contrast, the Bubble Phase, despite being spatially fragmented, maintains a cleaner spectral signature within its localized clusters. We therefore identify the high-hopping regime as an Unstable Superfluid (USF), distinct from the stable Bubble glass.

Combining these signatures, we confirm that the Bubble Phase resides precisely at the boundary between the MI and the USF phases. Notably, this phase structure—where a glassy state intervenes between the insulator and the superfluid—strikingly mirrors the “Bose glass” phase observed in models with explicit off-diagonal disorder [4]. This morphological similarity strongly suggests

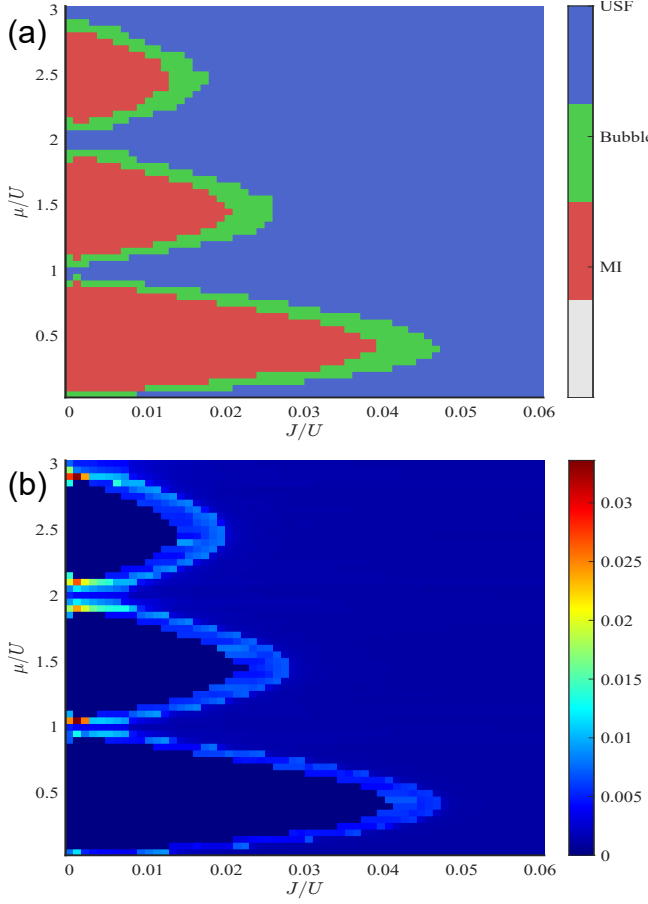


FIG. 1. **Ground-state phase diagram and coherence signatures for $\alpha = 1/16$.** (a) Phase diagram in the $(J/U, \mu/U)$ plane determined by the real-space connectivity of the superfluid order parameter. Three distinct phases are identified: the Mott Insulator (MI), the Unstable Superfluid (USF), and the intervening Bubble Phase, which emerges at the phase boundary due to spontaneous fragmentation. (b) Corresponding momentum-space coherence map quantified by the Inverse Participation Ratio (IPR), \mathcal{I}_k . The Bubble phase retains structural coherence (higher IPR) arising from its Bragg peaks, whereas the deep USF regime exhibits a suppressed IPR due to the proliferation of diffuse background modes, signaling dynamical instability.

that phase frustration acts as an intrinsic counterpart to random hopping, driving the system into a glass-like state even in the absence of extrinsic impurities.

DYNAMICAL STABILITY AND EXCITATION SPECTRUM

To verify the stability of the Bubble Phase, we investigate the collective excitation spectrum using the quantum Gutzwiller approach developed by Caleffi *et al.* [25]. Standard BdG approaches rely on expanding boson operators around a condensate mean-field, implicitly assum-

ing that the ground state satisfies the Gross-Pitaevskii equation to eliminate linear fluctuation terms. However, this assumption fails for the Gutzwiller wavefunction $|\Psi_G\rangle$, which possesses a complex local Fock space structure incompatible with a simple coherent state ansatz.

To resolve this, we adopt the slave-particle formalism where the Gutzwiller variational parameters are promoted to quantum operators $\hat{f}_{n,\mathbf{r}}$ satisfying bosonic commutation relations. The physical boson annihilation operator is reconstructed within the Gutzwiller basis as $\hat{b}_{\mathbf{r}} = \sum_n \sqrt{n} \hat{f}_{n-1,\mathbf{r}}^\dagger \hat{f}_{n,\mathbf{r}}$. We define the Nambu spinor of fluctuations at site \mathbf{r} as $\delta\hat{\Phi}_{\mathbf{r}} = (\delta\hat{f}_{0,\mathbf{r}}, \dots, \delta\hat{f}_{n_{max},\mathbf{r}}, \delta\hat{f}_{0,\mathbf{r}}^\dagger, \dots, \delta\hat{f}_{n_{max},\mathbf{r}}^\dagger)^T$. Linearizing the Heisenberg equations of motion $i\partial_t \delta\hat{\Phi}_{\mathbf{r}} = [\delta\hat{\Phi}_{\mathbf{r}}, \hat{H}]$ leads to the generalized BdG eigenvalue problem:

$$\mathcal{M}_{\text{BdG}} \mathbf{V}_\nu = \omega_\nu \mathbf{V}_\nu, \quad (4)$$

where \mathbf{V}_ν is the eigenvector corresponding to the mode frequency ω_ν . The dynamical matrix \mathcal{M}_{BdG} possesses the characteristic block structure enforced by Bose statistics:

$$\mathcal{M}_{\text{BdG}} = \begin{pmatrix} \mathcal{A} & \mathcal{B} \\ -\mathcal{B}^* & -\mathcal{A}^* \end{pmatrix}, \quad (5)$$

where the submatrices \mathcal{A} and \mathcal{B} are derived from the second-order variation of the energy functional with respect to the Gutzwiller parameters (explicit expressions are provided in the Appendix).

A critical challenge in this slave-particle formalism is the significant enlargement of the configuration space: the dimension of the BdG dynamical matrix increases from $2N$ in standard theory to $2N(n_{max} + 1)$. This expansion introduces a set of redundant, non-physical modes arising from the gauge degrees of freedom intrinsic to the Gutzwiller ansatz. As demonstrated by Caleffi *et al.* [25], these spurious modes are exact zero-energy eigenstates of the dynamical matrix. Consequently, they inevitably mix with physical low-energy excitations during numerical diagonalization, obscuring the true spectrum. To decouple the physical sector, we implement the Energy Penalty Method by constructing the effective dynamical matrix $\mathcal{M}_{\text{eff}} = \mathcal{M}_{\text{BdG}} + \Lambda \mathcal{P}_{\text{spur}}$. Here, $\mathcal{P}_{\text{spur}}$ is the projection operator onto the subspace spanned by these non-physical zero-energy modes, and $\Lambda \gg J$ is a large penalty parameter that shifts them to high energies, leaving the physical spectrum pristine.

The calculated excitation spectrum along a cut at fixed $\mu/U = 0.5$ is shown in Fig. 2. This scan traverses three distinct regimes:

(i) **Mott Insulator ($J/U \lesssim 0.04$):** The lowest excitation energy (blue solid line) is real and finite. It decreases linearly with increasing hopping, consistent with the perturbative softening of the Mott gap expected in the strong-coupling limit [2].

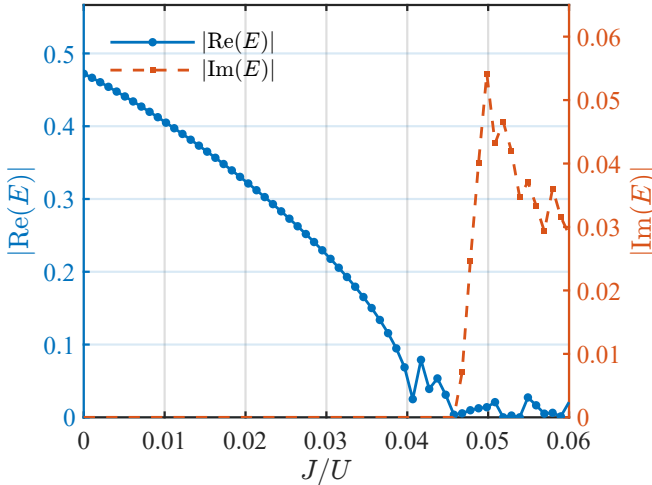


FIG. 2. Dynamical stability and excitation spectrum. Evolution of the lowest Bogoliubov-de Gennes (BdG) excitation energy as a function of hopping strength J/U (at fixed $\mu/U = 0.5$). The solid blue line represents the real energy gap $|\text{Re}(E)|$, while the dashed red line indicates the imaginary part $|\text{Im}(E)|$ associated with dynamical instability. The Bubble phase (for $J/U \lesssim 0.046$) is characterized by a purely real spectrum ($|\text{Im}(E)| = 0$) with a finite gap, confirming it is a stable eigenstate rather than a numerical artifact. The sudden rise in $|\text{Im}(E)|$ marks the transition into the Unstable Superfluid (USF) phase.

(ii) **Bubble Phase** ($0.04 \lesssim J/U \lesssim 0.046$): In this intermediate window, the spectrum remains strictly purely real ($|\text{Im}(E)| = 0$, red dashed line), providing definitive proof that the Bubble Phase is a dynamically stable eigenstate. Significantly, the system maintains a finite excitation gap, distinguishing it from the conventional gapless Bose glass. We attribute this gapped nature to the absence of Griffiths singularities: unlike random potentials that allow for arbitrarily large rare regions, the deterministic phase frustration imposes a structural regularity on the superfluid clusters, effectively truncating the low-energy spectrum.

(iii) **Unstable Superfluid** ($J/U \gtrsim 0.046$): Upon further increasing hopping, complex eigenvalues emerge ($|\text{Im}(E)| > 0$). In the BdG formalism, a complex frequency ω implies that fluctuations grow exponentially in time ($\sim e^{\text{Im}(\omega)t}$), explicitly signaling dynamical instability. This marks the breakdown of the stable Gutzwiller ground state and corresponds to the onset of the chaotic, unstable superfluid regime.

These spectral signatures explicitly validate the phase diagram in Fig. 1 and rigorously establish the Bubble Phase as a stable and gapped eigenstate of the frustrated Hamiltonian.

CHARACTERISTICS OF THE BUBBLE PHASE

Finally, we elucidate the physical characteristics of the Bubble Phase by combining its microscopic texture (Fig. 3) with its macroscopic bulk properties (Fig. 4).

A. Microscopic Origin: Spontaneous Fragmentation

The real-space structure of the order parameter $\psi_r = \langle \hat{b}_r \rangle$, shown in Fig. 3, provides the key to understanding the system's insulating behavior. Unlike the uniform Mott insulator [Fig. 3(a)] or the globally connected Superfluid, the Bubble Phase [Fig. 3(b)] spontaneously fragments into an array of localized superfluid islands separated by Mott-insulating domain walls.

This fragmentation arises directly from the competition between incompatible local phase configurations. A close inspection of the phase texture in Fig. 3(e) reveals the coexistence of distinct local patterns, including uniform, stripy, and checkerboard modulations. By comparing this with the amplitude map in Fig. 3(b), we find that the Mott insulating regions (where $|\psi_r| \rightarrow 0$) are located precisely at the interfaces between these distinct phase domains. This spatial correlation provides compelling evidence that the Mott barriers emerge specifically to resolve the conflicts between these mismatched phase configurations.

This picture of local coherence without global order is corroborated by the momentum-space distribution $n(\mathbf{k})$, displayed in the bottom row of Fig. 3. While the Mott phase [Fig. 3(g)] is featureless, the Bubble Phase [Fig. 3(h)] exhibits distinct Bragg peaks, reflecting the periodic arrangement of the superfluid clusters. However, under the same intensity scale, the peak intensity in the Bubble Phase is significantly weaker than that of the Unstable Superfluid [Fig. 3(i)]. This suppression of the condensate peak signifies the absence of true long-range off-diagonal order (ODLRO), distinguishing the state from a supersolid and confirming its glassy nature.

We find that the bubble periodicity scales as $\lambda \propto 1/\alpha$; consequently, a larger magnetic flux would compress the bubbles into closer proximity. Excessive densification reduces the insulating barriers, eventually triggering superfluid percolation that reconnects the lattice and drives the system into dynamical instability ($|\text{Im}(E)| > 0$). Therefore, we fix $\alpha = 1/16$ specifically to maintain a sufficient separation ($\lambda = 16a$) that suppresses percolation, ensuring the realization of a dynamically stable Bubble Phase with a purely real spectrum .

B. Macroscopic Signature: Compressible Insulator

The localized nature of the bubbles implies that the system, while globally insulating, retains local superfluid

susceptibility. This structure leads to a fundamental distinction from the incompressible Mott limit, as evidenced by the macroscopic observables in Fig. 4.

Figure 4(a) shows the equation of state (density n vs. chemical potential μ). While the Mott phase is characterized by an incompressible plateau ($\kappa = \partial n / \partial \mu = 0$), the Bubble Phase exhibits a continuously varying density with a finite slope, indicating a finite compressibility $\kappa > 0$. To make this explicit, we analyze the on-site particle number fluctuations $\langle \delta \hat{n}^2 \rangle = \langle \hat{n}^2 \rangle - \langle \hat{n} \rangle^2$ in Fig. 4(b). Based on the fluctuation-dissipation relation, the compressibility is linked to local density fluctuations. As shown in Fig. 4(b), while fluctuations are suppressed to zero in the Mott limit, the Bubble Phase exhibits a significant finite value. This confirms that within the superfluid bubbles, particles are delocalized and compressible, even if transport is blocked globally.

The coexistence of finite compressibility (locally superfluid) and global insulating behavior (lack of percolation due to domain walls) is the defining phenomenology of a Bose Glass. Unlike conventional Bose glasses induced by extrinsic randomness, here the glassy state emerges in a disorder-free setting, driven purely by deterministic phase frustration. We thus identify this state as an Intrinsic Bose Glass.

DISCUSSION

The emergence of the Bubble Phase in our frustrated Hamiltonian is not an isolated phenomenon but rather a specific manifestation of a generic mechanism driving frustration-induced localization. While the coexistence of superfluid clusters and insulating barriers is conventionally attributed to quenched disorder [2, 4, 5], our work demonstrates that it can be generically understood through a unified framework of phase frustration. This framework bridges the gap between disorder-driven phenomena and similar fragmented states arising from deterministic inhomogeneities, such as tunable weak links [26], off-diagonal confinement [27], twisted bilayer geometries [12], and even non-Hermitian models characterized by non-reciprocal phase factors [28]. To demystify the physical origin of this frustration, let us consider a generic bosonic system where the hopping amplitude t_{ij} is spatially modulated. Since the hopping connects two sites, its magnitude is naturally defined on the bond center $\mathbf{R}_{ij} = (\mathbf{r}_i + \mathbf{r}_j)/2$. Any such spatial texture $t(\mathbf{R}_{ij})$ can be decomposed via Fourier analysis into a spectrum of spatial frequencies:

$$t_{ij} = t(\mathbf{R}_{ij}) = \sum_{\mathbf{q}} \mathcal{T}_{\mathbf{q}} e^{i\mathbf{q} \cdot \mathbf{R}_{ij}}. \quad (6)$$

This decomposition offers a direct mapping to the standard Peierls substitution, $t_{ij} \sim e^{i\mathbf{A}(\mathbf{R}_{ij}) \cdot (\mathbf{r}_i - \mathbf{r}_j)}$, describing bosons in a gauge field. To see this explicitly, we

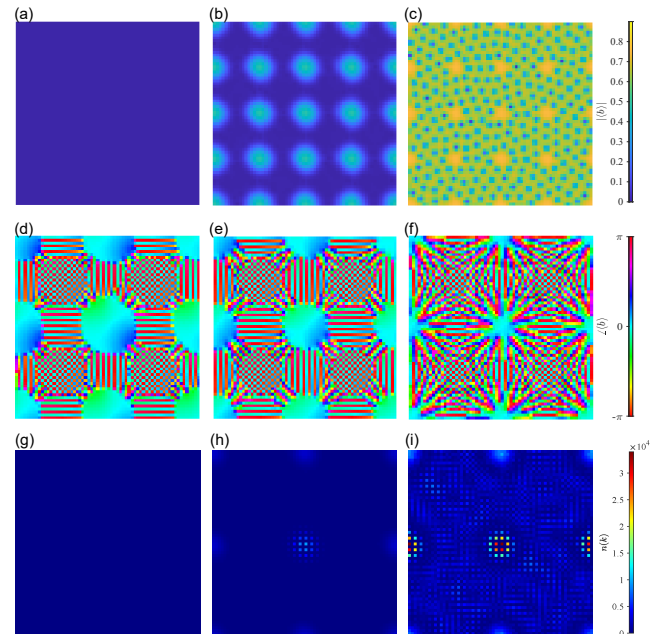


FIG. 3. Microscopic signatures of spontaneous fragmentation. Real-space distribution of the local superfluid order parameter amplitude $|\langle b_i \rangle|$ (top row), phase $\arg(\langle b_i \rangle)$ (middle row), and momentum space distribution $n(\mathbf{k})$ (bottom row) for three representative phases on a 64×64 lattice. **(a, d, g) Mott Insulator** ($J/U = 0.03$): The system exhibits a uniform vanishing amplitude and a featureless momentum distribution (intensity ≈ 0). **(b, e, h) Bubble Phase** ($J/U = 0.045$): The system spontaneously fragments into localized superfluid ‘islands’ (bubbles). Within each bubble, the phase is ordered, but global coherence is disrupted by the insulating domain walls. This is confirmed by the momentum distribution (h), which shows distinct Bragg peaks but with significantly reduced intensity compared to the superfluid phase, reflecting the lack of long-range ODLRO. **(c, f, i) Unstable Superfluid** ($J/U = 0.06$): The system regains global connectivity but displays chaotic patterns. The momentum distribution (i) shows strong but diffuse peaks, signaling the onset of dynamical instability.

define the bond vector $\boldsymbol{\delta} = \mathbf{r}_i - \mathbf{r}_j$ (assuming unit lattice spacing, $|\boldsymbol{\delta}| = 1$). For a fixed hopping direction $\boldsymbol{\delta}$, we can rewrite the spatial modulation phase using the identity $\mathbf{q} \cdot \mathbf{R}_{ij} = [(\mathbf{q} \cdot \mathbf{R}_{ij})\boldsymbol{\delta}] \cdot \boldsymbol{\delta}$. This allows us to identify an effective gauge potential:

$$\mathbf{A}_{\text{eff}}(\mathbf{R}_{ij}) \equiv (\mathbf{q} \cdot \mathbf{R}_{ij}) \boldsymbol{\delta}. \quad (7)$$

Substituting this back, we recover the Peierls form $\mathbf{q} \cdot \mathbf{R}_{ij} = \mathbf{A}_{\text{eff}}(\mathbf{R}_{ij}) \cdot (\mathbf{r}_i - \mathbf{r}_j)$. Since $\mathbf{A}_{\text{eff}}(\mathbf{R})$ is a linear function of the coordinates \mathbf{R} , it corresponds physically to a uniform magnetic field (where the vector potential grows linearly). Consequently, Eq. (6) implies that an arbitrary hopping texture involving multiple \mathbf{q} modes is equivalent to subjecting the boson to a superposition of distinct, competing magnetic fields. The boson is thus simultaneously driven by conflicting Gauge-imposed con-

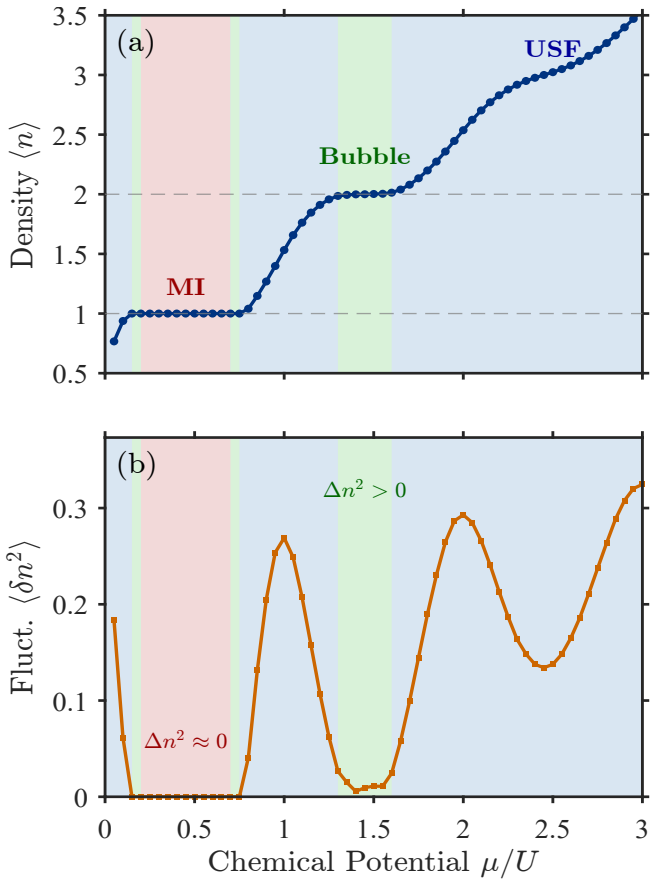


FIG. 4. Macroscopic bulk properties at fixed hopping $J/U = 0.025$. (a) Equation of state showing the average particle number $\langle n \rangle$ as a function of the chemical potential μ/U . The Mott Insulator (red shaded region) is characterized by an integer filling plateau where the compressibility vanishes ($\kappa = \partial n / \partial \mu \approx 0$). Conversely, the Bubble Phase (green shaded region) exhibits a continuously varying density with a finite slope, indicating a finite compressibility ($\kappa > 0$). (b) Particle number fluctuations $\langle \delta n^2 \rangle$. The Bubble Phase supports significant number fluctuations ($\langle \delta n^2 \rangle > 0$), distinguishing it from the particle-number-squeezed Mott state ($\langle \delta n^2 \rangle \approx 0$). These bulk properties identify the Bubble Phase as a compressible insulator.

straints, leading to severe phase frustration. To resolve this tension, the system spontaneously creates insulating domain walls to screen the conflicting phase gradients, resulting in the localized superfluid clusters (bubbles) we observe.

This perspective offers a fresh insight into the nature of the Bose Glass. Traditionally, the Bose Glass is viewed as a consequence of Anderson localization induced by diagonal disorder (random chemical potentials) [2]. However, in the context of off-diagonal disorder (random hopping amplitudes) [5], the physics is governed by the complex spatial texture of t_{ij} . Applying our Fourier analysis framework [Eq. (6)], a stochastic distribution of hopping

strengths corresponds to a broad, continuous spectrum of \mathbf{q} modes. Physically, this represents the limit of “extreme phase frustration,” where the boson is subjected to a turbulent superposition of random effective magnetic fields. Unable to satisfy this chaotic set of gauge-imposed constraints, the system’s global phase coherence shatters. To minimize energy, the superfluid fragments into a myriad of disjointed islands separated by insulating boundaries—phenomenologically identical to the state observed in our model. Our “Intrinsic Bose Glass,” generated here by deterministic phase frustration, thus serves as a pristine, disorder-free archetype of this universal mechanism, revealing that severe phase frustration alone is sufficient to drive the superfluid-to-glass transition.

This work utilizes the Energy Penalty Method to resolve numerical instabilities in the BdG spectrum.

* yangshijie@tsinghua.org.cn

- [1] P. W. Anderson, Phys. Rev. **109**, 1492 (1958).
- [2] M. P. A. Fisher, P. B. Weichman, G. Grinstein, and D. S. Fisher, Phys. Rev. B **40**, 546 (1989).
- [3] L. Fallani, J. E. Lye, V. Guarrera, C. Fort, and M. Inguscio, Phys. Rev. Lett. **98**, 130404 (2007).
- [4] P. Sengupta and S. Haas, Phys. Rev. Lett. **99**, 050403 (2007).
- [5] A. M. Piekarska and T. K. Kopeć, Phys. Rev. Lett. **120**, 160401 (2018).
- [6] A. M. Piekarska and T. K. Kopeć, Phys. Rev. B **105**, 174203 (2022).
- [7] A. Smith, J. Knolle, D. L. Kovrizhin, and R. Moessner, Phys. Rev. Lett. **118**, 266601 (2017).
- [8] P. Karpov, R. Verdel, Y.-P. Huang, M. Schmitt, and M. Heyl, Phys. Rev. Lett. **126**, 130401 (2021).
- [9] S. Aubry and G. André, Ann. Israel Phys. Soc. **3**, 133 (1980).
- [10] T. Roscilde, Phys. Rev. A **77**, 063605 (2008).
- [11] S.-H. Ding, L.-J. Lang, Q. Zhu, and L. He, Phys. Rev. A **112**, 033322 (2025).
- [12] C. Zhang, Z. Fan, B. Capogrosso-Sansone, and Y. Deng, Phys. Rev. B **111**, 024511 (2025).
- [13] M. Ciardi, A. Angelone, F. Mezzacapo, and F. Cinti, Phys. Rev. Lett. **131**, 173402 (2023).
- [14] S. Powell, R. Barnett, R. Sensarma, and S. D. Sarma, Phys. Rev. A **83**, 013612 (2011).
- [15] R. Sachdeva and S. Ghosh, Phys. Rev. A **85**, 013642 (2012).
- [16] A. Dhar, M. Maji, T. Mishra, R. V. Pai, S. Mukerjee, and A. Paramekanti, Phys. Rev. A **85**, 041602 (2012).
- [17] J. J. Slim, C. C. Wanjura, M. Brunelli, J. del Pino, A. Nunnenkamp, and E. Verhagen, Nature **627**, 767 (2024).
- [18] J. H. Busnaina, Z. Shi, A. McDonald, D. Dubyna, I. Nsanzineza, J. S. C. Hung, C. W. S. Chang, A. A. Clerk, and C. M. Wilson, Nat. Commun. **15**, 3065 (2024).
- [19] A. McDonald, T. Pereg-Barnea, and A. A. Clerk, Phys. Rev. X **8**, 041031 (2018).
- [20] S. Vishveshwara and D. M. Weld, Phys. Rev. A **103**, L051301 (2021).

- [21] Y.-N. Wang, W.-L. You, and G. Sun, Phys. Rev. A **106**, 053315 (2022).
- [22] P. Buonsante, F. Massel, V. Penna, and A. Vezzani, Phys. Rev. A **79**, 013623 (2009).
- [23] K. Suthar, H. Sable, R. Bai, S. Bandyopadhyay, S. Pal, and D. Angom, Phys. Rev. A **102**, 013320 (2020).
- [24] J. Hoshen and R. Kopelman, Phys. Rev. B **14**, 3438 (1976).
- [25] F. Caleffi, M. Capone, C. Menotti, I. Carusotto, and A. Recati, Phys. Rev. Research **2**, 033276 (2020).
- [26] K. Hettiarachchilage, V. G. Rousseau, K.-M. Tam, M. Jarrell, and J. Moreno, Phys. Rev. A **87**, 051607 (2013).
- [27] G. J. Cruz, R. Franco, and J. Silva-Valencia, J. Phys.: Conf. Ser. **480**, 012003 (2014).
- [28] X.-r. Zhang and S.-J. Yang, Results Phys. **53**, 106998 (2023).

Supplementary Material for: Phase Frustration Induced Intrinsic Bose Glass in the Kitaev-Bose-Hubbard Model

A. Explicit Form of the BdG Dynamical Matrix in Slave-Particle Formalism

In this section, we provide the explicit expressions for the matrix elements of the Bogoliubov-de Gennes (BdG) dynamical matrix \mathcal{M}_{BdG} derived within the slave-particle formalism.

As introduced in the main text, the fluctuation operators are defined via the slave particles $\hat{c}_{n,i}$, where $\hat{b}_i = \sum_n \sqrt{n} \hat{c}_{n,i}^\dagger \hat{c}_{n-1,i}$. The BdG Hamiltonian in the Nambu basis $\delta\hat{\Phi} = (\delta\hat{c}, \delta\hat{c}^\dagger)^T$ takes the block form:

$$\mathcal{M}_{\text{BdG}} = \begin{pmatrix} \mathbf{A} & \mathbf{B} \\ -\mathbf{B}^* & -\mathbf{A}^* \end{pmatrix}. \quad (\text{S1})$$

Here, the indices of the submatrices run over (i, m) and (j, n) , representing the m -th Fock state at site i and the n -th Fock state at site j , respectively. The hopping amplitude is denoted by J , the pairing amplitude by Δ , and the Peierls phase by θ_{ij} . We assume the pairing phase follows the gauge field $(\phi_{ij} = \theta_{ij})$.

The mean-field parameters are defined based on the local ground state coefficients $c_{n,i}^{(0)}$:

$$\begin{aligned} \psi_i &= \sum_n \sqrt{n} c_{n-1,i}^{(0)*} c_{n,i}^{(0)}, \\ \bar{n}_i &= \sum_n n |c_{n,i}^{(0)}|^2, \\ \overline{n(n-1)}_i &= \sum_n n(n-1) |c_{n,i}^{(0)}|^2. \end{aligned} \quad (\text{S2})$$

1. Matrix **A** (Normal Terms)

The matrix **A** contains diagonal and off-diagonal terms associated with particle number conservation (in the hopping sector) and anomalous mixing (in the pairing sector).

On-site Diagonal Elements ($i = j, m = n$): These terms describe the local energy cost including interaction, chemical potential, and the mean-field energy shift from neighbors:

$$\begin{aligned} A_{im,im} &= \frac{U}{2} [m(m-1) - \overline{n(n-1)}_i] - \mu(m - \bar{n}_i) \\ &+ \sum_{j \in \text{NN}(i)} 2 \text{Re} [e^{i\theta_{ij}} (J\psi_j \psi_i^* + \Delta \psi_i^* \psi_j^*)]. \end{aligned} \quad (\text{S3})$$

On-site Off-diagonal Elements ($i = j, n = m - 1$): These terms arise from the coupling to the mean-field order parameter:

$$\begin{aligned} A_{i,m,m-1} &= -\sqrt{m} \sum_{j \in \text{NN}(i)} \left[J(e^{i\theta_{ij}} \psi_j + e^{-i\theta_{ij}} \psi_j^*) \right. \\ &\quad \left. + \Delta(e^{i\theta_{ij}} \psi_j^* + e^{-i\theta_{ij}} \psi_j) \right]. \end{aligned} \quad (\text{S4})$$

Note that Hermiticity of the block **A** implies $A_{i,m-1,m} = A_{i,m,m-1}^*$.

Off-site Elements ($i \neq j$): These terms describe the direct transfer or pairing of fluctuations between sites:

$$\begin{aligned} A_{im,jn} &= -J \left[e^{i\theta_{ij}} \sqrt{m n} c_{m-1,i}^{(0)} c_{n-1,j}^{(0)*} \right. \\ &\quad \left. + e^{-i\theta_{ij}} \sqrt{(m+1)(n+1)} c_{m+1,i}^{(0)} c_{n+1,j}^{(0)*} \right] \\ &\quad - \Delta \left[e^{i\theta_{ij}} \sqrt{m(n+1)} c_{m-1,i}^{(0)} c_{n+1,j}^{(0)*} \right. \\ &\quad \left. + e^{-i\theta_{ij}} \sqrt{n(m+1)} c_{n-1,j}^{(0)*} c_{m+1,i}^{(0)} \right]. \end{aligned} \quad (\text{S5})$$

2. Matrix **B** (Anomalous Terms)

The matrix **B** describes the creation/annihilation of pairs of fluctuations.

On-site Elements:

$$B_{im,in} = 0. \quad (\text{S6})$$

Off-site Elements ($i \neq j$):

$$\begin{aligned} B_{im,jn} = -J & \left[e^{i\theta_{ij}} \sqrt{m(n+1)} c_{m-1,i}^{(0)} c_{n+1,j}^{(0)} \right. \\ & + e^{-i\theta_{ij}} \sqrt{n(m+1)} c_{n-1,j}^{(0)} c_{m+1,i}^{(0)} \left. \right] \\ & - \Delta \left[e^{i\theta_{ij}} \sqrt{m n c_{m-1,i}^{(0)} c_{n-1,j}^{(0)}} \right. \\ & \left. + e^{-i\theta_{ij}} \sqrt{(m+1)(n+1)} c_{m+1,i}^{(0)} c_{n+1,j}^{(0)} \right]. \end{aligned} \quad (\text{S7})$$

The eigenvalues ω_ν of \mathcal{M}_{BdG} yield the collective excitation spectrum. The presence of any complex eigenvalue with $\text{Im}(\omega_\nu) \neq 0$ signals dynamical instability.

B. Perturbative Justification of the Energy Penalty Method

In the slave-particle formalism, the Hilbert space is enlarged, introducing a set of spurious zero-energy modes arising from the local $U(1)$ gauge symmetry and normalization constraints. These modes satisfy $\mathcal{M}_{\text{BdG}} |\Psi_{\text{spur}}\rangle = 0$. To decouple them from the physical spectrum, we construct an effective Hamiltonian $\mathcal{H}_{\text{eff}} = \mathcal{M}_{\text{BdG}} + \Lambda \mathcal{P}_{\text{spur}}$, where $\mathcal{P}_{\text{spur}}$ is the projection operator onto the spurious subspace and Λ is a large penalty parameter.

Here, we provide a rigorous justification based on standard perturbation theory (specifically, the projection technique for effective Hamiltonians). We demonstrate that, within a perturbative expansion in powers of $1/\Lambda$, this method effectively isolates physical modes with a vanishingly small energy shift, even in the presence of non-Hermitian couplings.

1. Block Hamiltonian Formalism

Let \hat{P} and \hat{Q} be the projection operators onto the low-energy physical subspace and the high-energy spurious subspace, respectively, satisfying $\hat{P} + \hat{Q} = \hat{1}$, $\hat{P}\hat{Q} = 0$, and importantly $\hat{Q} \equiv \mathcal{P}_{\text{spur}}$. The eigenvalue problem $\mathcal{H}_{\text{eff}} |\Psi\rangle = E |\Psi\rangle$ can be decomposed into block matrix form:

$$\begin{pmatrix} \hat{H}_{PP} & \hat{H}_{PQ} \\ \hat{H}_{QP} & \hat{H}_{QQ} \end{pmatrix} \begin{pmatrix} |\Psi_P\rangle \\ |\Psi_Q\rangle \end{pmatrix} = E \begin{pmatrix} |\Psi_P\rangle \\ |\Psi_Q\rangle \end{pmatrix}, \quad (\text{S8})$$

where $\hat{H}_{PP} = \hat{P} \mathcal{M}_{\text{BdG}} \hat{P}$ represents the intrinsic physics, while $\hat{H}_{QQ} = \hat{Q} (\mathcal{M}_{\text{BdG}} + \Lambda) \hat{Q}$ dominates the high-energy sector due to the large penalty Λ . We emphasize that due to the complex Peierls phases in the Kitaev-Bose-Hubbard model, the Hamiltonian is generally non-Hermitian, implying $\hat{H}_{PQ} \neq \hat{H}_{QP}^\dagger$.

2. Derivation of the Effective Hamiltonian

Expanding Eq. (S8) yields two coupled equations:

$$(E - \hat{H}_{PP}) |\Psi_P\rangle = \hat{H}_{PQ} |\Psi_Q\rangle, \quad (\text{S9})$$

$$(E - \hat{H}_{QQ}) |\Psi_Q\rangle = \hat{H}_{QP} |\Psi_P\rangle. \quad (\text{S10})$$

Assuming we are interested in the physical energy scale ($E \sim J, U \ll \Lambda$), the operator $(E - \hat{H}_{QQ})$ is invertible. We can express the spurious component as $|\Psi_Q\rangle = (E - \hat{H}_{QQ})^{-1} \hat{H}_{QP} |\Psi_P\rangle$. Substituting this back, we obtain an

energy-dependent effective Hamiltonian for the physical sector:

$$\mathcal{H}_{\text{phys}}(E) = \hat{H}_{PP} + \hat{H}_{PQ} \frac{1}{E - \hat{H}_{QQ}} \hat{H}_{QP}. \quad (\text{S11})$$

Since the penalty Λ is the dominant energy scale, the inverse operator (Green's function) can be expanded perturbatively:

$$\frac{1}{E - \hat{H}_{QQ}} \approx \frac{1}{E - (E_{\text{spur}} + \Lambda)} \approx -\frac{1}{\Lambda} + \mathcal{O}\left(\frac{1}{\Lambda^2}\right). \quad (\text{S12})$$

Substituting this approximation, the effective physical Hamiltonian becomes:

$$\mathcal{H}_{\text{phys}} \approx \hat{H}_{PP} - \frac{\hat{H}_{PQ} \hat{H}_{QP}}{\Lambda}. \quad (\text{S13})$$

This result reveals that the contamination from the spurious sector introduces an energy shift to the physical eigenvalues:

$$\delta E_{\text{phys}} \approx -\frac{\langle \Psi_P | \hat{H}_{PQ} \hat{H}_{QP} | \Psi_P \rangle}{\Lambda}. \quad (\text{S14})$$

Crucially, this shift scales as $1/\Lambda$. Even in our non-Hermitian system, the magnitude of this perturbative correction is strictly controlled by Λ . Therefore, by choosing $\Lambda \gg \max(J, U)$, the spurious modes are pushed to high energies while the physical spectrum remains asymptotically exact, validating the stability analysis presented in the main text.